

N. Hamm, P. M. Atkinson and E. J. Milton, "The combined effect of spatial resolution and measurement uncertainty on the accuracy of empirical atmospheric correction" *Proceedings of the the 2003 IEEE International Geoscience and Remote Sensing Symposium*, Centre de Congres Pierre Baudis, 21–25 July 2003.

**Copyright (c) 2003 IEEE.**

Reprinted from the Proceedings of the 2003 IEEE International Geoscience and Remote Sensing Symposium. 21-25 July 2003. Centre de Congres Pierre Baudis, Toulouse, France.

This material is posted here with permission of the IEEE. Such permission of the IEEE does not in any way imply IEEE endorsement of any of the University of Southampton's products or services. Internal or personal use of this material is permitted. However, permission to reprint/republish this material for advertising or promotional purposes or for creating new collective works for resale or redistribution must be obtained from the IEEE by writing to [pubs-permissions@ieee.org](mailto:pubs-permissions@ieee.org).

By choosing to view this document, you agree to all provisions of the copyright laws protecting it.

0-7803-7930-6/\$17.00 (C) 2003 IEEE

# The combined effect of spatial resolution and measurement uncertainty on the accuracy of empirical atmospheric correction

Nick Hamm, Peter M. Atkinson and Edward J. Milton

Department of Geography, University of Southampton, Southampton SO17 1BJ, UK

Email: nick@hamm.org; pma@soton.ac.uk; ejm@soton.ac.uk

**Abstract**—The combined effect of positional uncertainty of field data and pixel size on the accuracy of the empirical line method is examined and quantified. Positional uncertainty reduces accuracy, although this effect decreases as sample size and pixel size increases. For a pre-defined accuracy requirement, this information is used to specify the sample size required for a given pixel size.

## I. INTRODUCTION

The empirical line method (ELM) is used widely for the atmospheric correction of remotely sensed data from at-sensor radiance to at-surface reflectance. The ELM is based on a simple, first-order linear regression model where field-based measurements of reflectance are the dependent variable and remotely sensed measurements of radiance are the predictor variable. The field-based measurements are made using a radiometer or spectrometer to characterise the reflectance of a predefined selection of ground targets. These are combined with spatially coincident airborne measurements of radiance and the data set is used to estimate the parameters of the regression model. The estimated parameters are then used to predict at-surface reflectance over the remainder of the image [1].

A sufficiently large sample is required to allow accurate parameterisation of the regression model [1], [2]. The implementation also requires that the field measurements can be accurately located within the image. The possibility that uncertain location may lead to inaccurate parameterisation of the regression model is noted in the literature [3], [4]. However, the impact of this effect has received limited attention [5]. This research examines the effect of positional uncertainty in the field measurements for a range of sample sizes and pixel sizes. Specifically this research addresses two hypotheses:

- 1) that the model (ELM) uncertainty induced by positional uncertainty increases as the sample size decreases;
- 2) that the model (ELM) uncertainty induced by positional uncertainty decreases as the pixel size increases.

## II. FIELD SITE

Thorney Island in West Sussex, south east England contains a disused airfield with a range of surface cover types. These include asphalt, concrete and cropped grass, which are considered to be "typical" ground targets for use with the ELM [1]. On 24th July 2001 the site was overflowed by the Natural Environmental Research Council (NERC) aircraft which carried the Airborne Thematic Mapper (ATM). Data

were acquired at an altitude of approximately 1000 m on a north-to-south flight line oriented along the centre of the main runway. The field measurements were taken close to the centre of the image swath. This gave a basic pixel size of 2 m.

## III. METHOD

### A. Field measurements

Field measurements were taken on a nested square grid using a Milton Multiband Radiometer (MMR) [6] operating in dual beam mode [7]. This allowed straightforward processing to yield a reflectance factor  $\rho$  (%). The MMR samples the electromagnetic spectrum in four broad wavebands that correspond well with the ATM bands. The MMR is simple to use and allows near-instantaneous measurements to be made, making it ideal for acquisition of a spatially distributed large sample (approximately 230 observations per target). For this paper, analysis and discussion focuses on deriving broad-band reflectance for band 1 of the MMR (420–530 nm) using band 2 from the ATM (450–520 nm).

The location of each measurement was surveyed and recorded relative to UK Ordnance Survey (OS) trigonometric points. The ATM data were also geometrically corrected to the OS National Grid (RMSE < 1 pixel). This allowed each field measurement to be located within the image. Careful attention was given to ensuring that the location of the field measurements were recorded rigorously and precisely, both relative to each other and to the OS National Grid. In an operational situation, it might not be possible to record location with such rigour and precision and this research seeks to examine the implication of that. However, the analysis assumes that the geometric correction of the imagery is perfect.

### B. Simulating positional uncertainty

In order to simulate positional uncertainty a random error term was added to the location of each field measurement:

$$\begin{aligned}x_i &= \text{Easting} + \varepsilon_{x_i} \\y_i &= \text{Northing} + \varepsilon_{y_i}\end{aligned}\quad (1)$$

where  $i$  refers to each individual field location and  $\varepsilon$  is an error term drawn from a Normal distribution. The case where the user cannot give priority to recording location is represented as  $\varepsilon \sim N(E(0, 4))$  [5]. One thousand realisations of the sampling scheme for each surface were simulated and used to explore the effect on parameter estimation when implementing the ELM. These are termed the "perturbed" data sets.

### C. Implementing the ELM

Each field measurement was linked with its spatially coincident pixel value, yielding a set of data pairs. These were used for parameter estimation in the regression model. The normal error regression model is defined as:

$$\rho_i = \alpha + \beta \text{DN}_i + \varepsilon_i \quad (2)$$

where DN is the digital number from the image pixel,  $i$  refers to a specific data pair and  $\varepsilon_i \sim N(0, \sigma^2)$ . The point estimates are given as  $\hat{\alpha}$ ,  $\hat{\beta}$  and  $\hat{\sigma}^2$ . The full data set ( $nFull$ ) comprises 696 measurements ( $\sim 230$  per site). This was sub-sampled to examine the impact of sample size on parameter estimation, in the presence of positional uncertainty. Sub-samples of 100 ( $n100$ ), 50 ( $n50$ ), 30 ( $n30$ ), 20 ( $n20$ ), 10 ( $n10$ ), 5 ( $n5$ ), 3 ( $n3$ ) and 1 ( $n1$ ) measurements per site were created. Note that  $n1 \subset n3 \subset \dots \subset n100$ .

In order to examine the impact of pixel size, the image was degraded from 2 m pixels and the experiment repeated for 4 m, 6 m and 8 m pixel sizes.

## IV. RESULTS

### A. The full data set

The first stage was to examine the impact of positional uncertainty on parameter estimation using the full data set and 2 m pixels. The result of estimating the parameters of the regression model for 1000 perturbed data-set are shown in Figure 1. This clearly shows that the estimates of  $\hat{\alpha}$  and  $\hat{\sigma}^2$  are positively skewed, relative to the estimate made in the absence of positional uncertainty. The estimates of  $\hat{\beta}$  are negatively skewed. The increase in the value of  $\hat{\sigma}^2$  is indicative of the increase in uncertainty, both in parameter estimation and for prediction. It should be noted that the magnitude of the variability in  $\hat{\alpha}$  and  $\hat{\beta}$  is small in magnitude.

### B. The effect of reducing the sample size

The next stage was to examine the impact of positional uncertainty for the sub-sampled data-sets. This is illustrated in Figure 2 for the 2 m pixels. It is clear that the range of variation in the parameter estimates, in the presence of positional uncertainty, increases as the sample size decreases. This is particularly apparent where less than 20 measurements are made per target.

### C. The effect of increasing the pixel size

The next stage was to examine the impact of increasing the pixel size whilst holding the sample size fixed. The effect is illustrated in Figure 3 for  $\hat{\beta}$ . This figure, together with other results (not shown) lend weight to the hypothesis that the model uncertainty imposed by positional uncertainty decreases as the pixel size increases. However, there is an interesting twist here. For samples sizes that are lower than 100 per target, the variation in  $\hat{\beta}$  (as indicated by the standard deviation or the interquartile range) is larger for the 6 m pixels than for the 4 m pixels. The reason for this is unclear, but it is proposed that this may be due to the scale of spatial variation in the ground targets. For 6 m pixels neighbouring pixels may

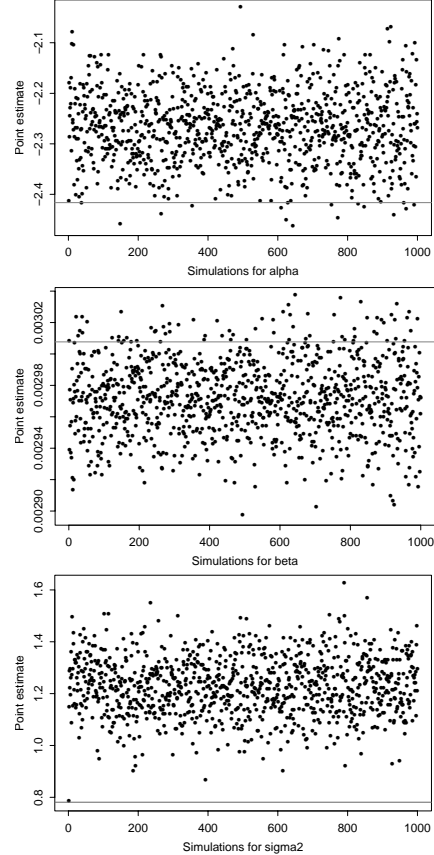


Fig. 1. Graphs showing the impact of positional uncertainty on parameter estimation for the full dataset. The horizontal line is the point estimate in the absence of positional uncertainty.

be more dissimilar than neighbouring pixels in the 4 m or 2 m pixel image. Hence the effect of introducing positional uncertainty is larger. For all sample sizes, the magnitude of variation for the 8 m pixels is lower than for the 4 m pixels.

## V. DISCUSSION

These results are of consequence, because they lead to variability in the parameter estimates. The value of  $\hat{\sigma}^2$  is informative because it allows quantification of uncertainty in estimation and prediction. However, variability in  $\hat{\alpha}$  and  $\hat{\beta}$  will concern the practitioner, since they affect the predicted value of reflectance. This is illustrated in Figure 4. This shows the regression line for the full dataset and 2 m pixels ( $\hat{\alpha} = -2.4164$ ,  $\hat{\beta} = 0.003007$ ) together with the line for  $\hat{\beta} \pm 0.0001$ . For a DN of 6000 this gives a range from 15.03 to 16.23 % but for a DN of 3000 a range from 6.31 to 6.91 %. The standard deviation ( $sd(\cdot)$ ) of the 1000 simulations is calculated and  $mean(\hat{\beta}) \pm 2 \times sd(\hat{\beta})$  was used as an uncertainty criterion. To achieve  $mean(\hat{\beta}) \pm 0.0001$  required a sample size of 50 measurements per target for the 2 m pixels, but only 30 measurements for the 4 m pixels and 20 measurements for the 8 m pixels. Applying the same approach to  $\alpha$ : to achieve  $mean(\hat{\alpha}) \pm 1$  required 20 measurements for the 2 m pixels, 10 for the 6 m pixels and 5 for the 8 m pixels.

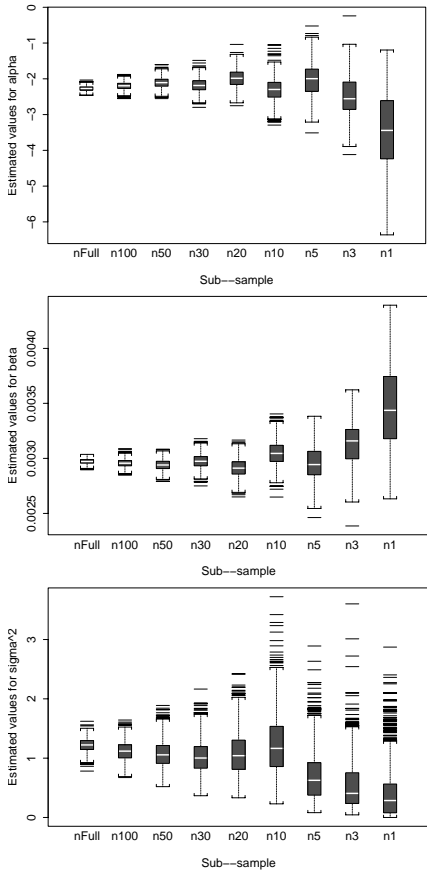


Fig. 2. Box-plots showing the impact of positional uncertainty on parameter estimation for 9 different sample sizes (see text).

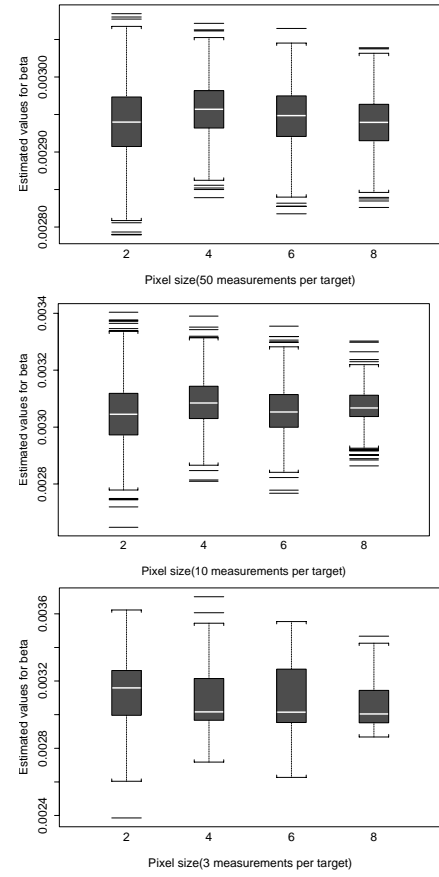


Fig. 3. The top (middle) (lower) panel shows the range of values for  $\hat{\beta}$  for 50 (10) (3) measurements per target, for different pixel sizes.

## VI. CONCLUSION

The research presented in this paper demonstrated the impact of positional uncertainty in field data on the estimation of the parameters of the regression line in the ELM. The impact was shown to be reduced as the pixel size or sample size increased. It was shown that this approach allows the sample size and/or pixel size to be selected on the basis of criteria relating to the uncertainty in the parameter estimation.

## ACKNOWLEDGMENT

This research is supported by a UK Natural Environmental Research Council (NERC) studentship (GT 04/99/FS/253) to N. Hamm. The NERC Airborne Remote Sensing Facility provided remotely sensed data. The NERC Equipment Pool for Field Spectroscopy provided field equipment and advice.

## REFERENCES

- [1] G. M. Smith and E. J. Milton, "The use of the empirical line method to calibrate remotely sensed data to reflectance," *Int. J. Remote Sensing*, vol. 20, no. 13, pp. 2653–2662, 1999.
- [2] E. Karpouzli and T. Malthus, "The empirical line method for the atmospheric correction of IKONOS imagery," *Int. J. Remote Sensing*, vol. 24, no. 5, pp. 1143–1150, 2003.
- [3] G. Ferrier, "Evaluation of apparent surface reflectance estimation methodologies," *Int. J. Remote Sensing*, vol. 17, no. 12, pp. 2291–2297, 1995.

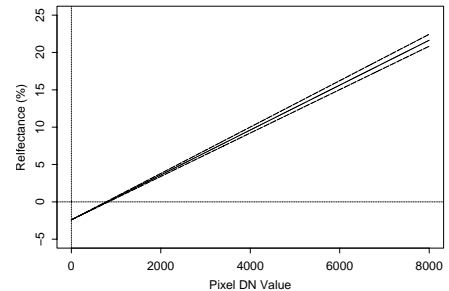


Fig. 4. Shows the estimated regression line for the full data set and 2 m pixels (thick line). The dashed lines show the regression line for  $\hat{\beta} \pm 0.0001$ .

- [4] G. Ferrier and G. Wadge, "The application of imaging spectrometry data to mapping alteration zones associated with gold mineralization in southern Spain," *Int. J. Remote Sensing*, vol. 16, no. 2, pp. 331–350, 1996.
- [5] N. Hamm, P. M. Atkinson, and E. J. Milton, "Evaluating the effect of positional uncertainty in field measurements on the atmospheric correction of remotely sensed imagery," in *geoENV IV – Geostatistics for Environmental Applications*, X. Sanchez-Vila and J. Carrera, Eds., London: Kluwer, in press.
- [6] E. J. Milton, "A portable multiband radiometer for ground data collection in remote sensing," *Int. J. Remote Sensing*, vol. 1, no. 2, pp. 153–165, 1980.
- [7] ———, "Principles of field spectroscopy," *Int. J. Remote Sensing*, vol. 8, no. 12, pp. 1807–1827, 1987.